第 49 卷 第 8 期 自 动 化 学 报 Vol. 49, No. 8
2023 年 8 月 ACTA AUTOMATICA SINICA August, 2023

基于自适应多尺度超螺旋算法的无人机集群姿态同步控制

蔡运颂 [1,2] 许 璟 [1,2] 牛玉刚 [1,2]

摘 要 四旋翼无人机 (Unmanned aerial vehicle, UAV) 系统姿态角和角速度分别为运行在不同时间尺度上的慢、快动态. 由于输入扰动的上界难以精确估计, 本文提出一种基于自适应多尺度超螺旋 (Super-twisting, STW) 滑模算法的无人机集群一致性控制策略. 首先, 建立无人机集群系统的姿态角模型, 并通过奇异摄动理论将其化为两时间尺度形式. 基于系统的快慢特性, 本文设计两时间尺度的超螺旋滑模算法, 并采用自适应增益处理无人机集群系统的未知边界非线性. 此外, 还提出一种改进型自适应多尺度超螺旋滑模算法, 进一步减少系统的一致性收敛时间, 实现无人机集群姿态角有限时间内同步. 最后通过仿真分析, 验证两种自适应多尺度超螺旋算法的正确性和有效性.

关键词 奇异摄动, 超螺旋算法, 多尺度, 姿态协同, 四旋翼无人机

引用格式 蔡运颂, 许璟, 牛玉刚. 基于自适应多尺度超螺旋算法的无人机集群姿态同步控制. 自动化学报, 2023, **49**(8): 1656−1666

DOI 10.16383/j.aas.c220759

Attitude Consensus Control of UAV Swarm Based on Adaptive Multi-scale Super-twisting Algorithm

CAI Yun-Song[1,2] XU Jing[1,2] NIU Yu-Gang[1,2]

Abstract In a UAV (unmanned aerial vehicle) system, the attitude angle and angular velocity of the UAV are, respectively, the slow and fast dynamics operating in different time scales. Due to the difficulty in the estimation of the bound of disturbance, this paper proposes a control method for UAV swarm, based on the adaptive multi-scale STW (super-twisting) sliding mode algorithm. First, the attitude model of the UAV swarm system is established, which is transformed into a two-time-scale model via singular perturbation theory. On this basis, this paper designs a two-time-scale STW sliding mode algorithm with adaptive gains to deal with the perturbations and unknows. Furthermore, by adding a few linear iterms, a modified adaptive STW control algorithm is also provided, which further reduces the convergence time and achieves the synchronization of the attitudes in finite time. Finally, the effectiveness of two different adaptive multi-scale STW algorithms are verified through simulations.

Key words Singular perturbation, STW, multi-scale, attitude coordination, quadrotors

Citation Cai Yun-Song, Xu Jing, Niu Yu-Gang. Attitude consensus control of UAV swarm based on adaptive multi-scale super-twisting algorithm. *Acta Automatica Sinica*, 2023, **49**(8): 1656−1666

四旋翼无人机[1−2](Unmanned aerial vehicle, UAV) 具有结构简单、飞行精准、机动性强等优点. 因此, 在军事打击[3−4]、载物[5−6]、测量[7−8]、灾害监测[9]等方面, 有着很好的应用. 然而随着控制任务复杂度的增加, 例如无人机表演[10]、沿海侦察、集群打击等, 仅凭一台无人机难以完成, 因此需要多台无人机集群协同作业. 在对四旋翼无人机进行建模时, 通常简单地认为无人机模型是单一尺度的. 然而实际上, 无人机的姿态角与角速度并不处于同一时间尺度, 这是由无人机中的参数量纲差异引起的. 因此, 无人机集群的奇异摄动建模具有重要意义, 通过奇异摄动建模可以抽提出无人机状态的快慢特性. 然而, 对于奇异摄动无人机集群系统而言, 基于单一时间尺度的控制策略效果欠佳.

目前, 四旋翼无人机集群控制方法主要有反步法、模糊控制以及 PID (Proportion-integral-derivative) 控制方法等. 文献 [11] 针对多四旋翼无人机的编队控制, 采用反步法实现了四旋翼无人机群对期望轨迹的跟踪功能. 文献 [12] 建立了四旋翼无人机的姿态动力学模糊模型, 设计了模糊反馈控制器,

收稿日期 2022-09-22 录用日期 2023-02-10
Manuscript received September 22, 2022; accepted February 10, 2023
国家自然科学基金 (62173141, 62073139), 上海市自然科学基金 (22ZR1417900) 资助
Supported by National Natural Science Foundation of China (62173141, 62073139) and the Natural Science Foundation of Shanghai (22ZR1417900)
本文责任编委 李鸿一
Recommended by Associate Editor LI Hong-Yi
1. 华东理工大学信息科学与工程学院 上海 200237 2. 华东理工大学能源化工过程智能制造教育部重点实验室 上海 200237
1. College of Information Science and Engineering, East China University of Science and Technology, Shanghai 200237 2. Key Laboratory of Intelligent Manufacturing of Energy and Chemical Processes of Ministry of Education, East China University of Science and Technology, Shanghai 200237

实现了四旋翼无人机集群控制. 文献 [13] 设计了一种 BP (Back propagation) 神经网络辅助的 PID 无人机编队智能算法, 实现了 PID 参数的优化整定[14]. 对四旋翼无人机集群的研究中, 姿态协同是四旋翼无人机群实现队形控制、协同避障等任务的基础. 文献 [15] 基于半定规划进行迭代区域扩张完成了多无人机的队形设计. 文献 [16] 利用神经网络预测姿态偏差, 将其集成于分散式容错协同控制器中, 实现了姿态角的一致性. 然而, 考虑到无人机的动态模型中存在着内部结构不确定, 外界扰动影响等问题, 导致基于无扰动简化模型的控制方案效果有限.

在姿态协同控制中, 滑模控制是一类有效的鲁棒控制方法, 对于外部输入扰动或者参数不确定性具有不变性、有限时间可达等优点. 目前, 滑模控制方法大致可以分为一阶滑模与高阶滑模. 如文献 [17] 基于一阶滑模与低通滤波器的结合, 实现了对直流电机位置的控制. 然而, 一阶滑模是直接基于滑模变量的一阶导数设计的, 采用了切换控制律, 产生了严重的抖振现象, 影响系统性能. 在二阶滑模算法中, 超螺旋滑模算法 (Super-twisting, STW) 的应用最为广泛. 这是由于超螺旋滑模控制器采用了连续控制结构, 引入了积分项, 避免了使用切换项 sgn(·), 响应速度快, 对抖振抑制能力强, 并且可以驱使滑模变量及其导数在有限时间内收敛到稳定点. 同时, 能够处理上界为依赖于状态的函数以及符合 Lipschitz 条件[18] 的扰动. 文献 [19] 采用了超螺旋滑模控制策略, 提高了永磁同步电机的转速响应. 文献 [20] 提出了一种基于超螺旋滑模的干扰观测器, 实现了对未估计的干扰的精细化补偿. 然而上述滑模控制方法都是基于已知上界的非线性, 这在无人机中是无法实现的.

为了实现姿态协同的稳准快, 本文设计了一种新型的分尺度自适应 STW 算法, 通过分尺度自适应 STW 控制器产生的不同时间尺度上的快、慢控制律, 实现了四旋翼无人机奇异摄动多智能体模型中的分尺度精确控制. 同时, 通过自适应增益实现扰动未知情况下的快速补偿. 与现有部分研究成果相比, 本文的主要贡献归纳为如下几个方面:

1) 多时间尺度超螺旋控制结构: 本文提出了多时间尺度超螺旋滑模控制器的设计方法, 在控制器中引入两个时间尺度, 通过奇异摄动方法来有效处理四旋翼无人机姿态角系统状态同步问题.

2) 自适应分布式控制器: 本文采用了分布式的控制结构, 对每个四旋翼无人机智能体分别设计了一个自适应增益, 让其自适应于四旋翼无人机智能体本身以及与其他智能体间的耦合.

符号描述. 对于一个 $n\times n$ 维的矩阵 X, 上标 -1 表示矩阵的逆, 上标 T 表示矩阵的转置, $\otimes$ 表示矩阵的克罗内克积, $\mathrm{diag}\{a_1, a_2, a_3\}$ 表示对角线上的元素为 a_1, a_2, a_3 的矩阵. 对于一个 n 维向量 $\boldsymbol{b}$, 上标 T 表示向量的转置, sgn 表示符号函数, $\mathrm{col}\{\boldsymbol{b}_1, \boldsymbol{b}_2, \boldsymbol{b}_3\}$ 表示向量按列排序, $|\boldsymbol{b}|$ 表示 $\boldsymbol{b}$ 内元素取绝对值后的向量, $||\boldsymbol{b}||$ 表示向量的二范数, $\boldsymbol{b}^{\frac{1}{2}}$ 表示 $\boldsymbol{b}$ 内元素开根号后的向量. $\min(\omega)$ 表示取集合 ω 中最小的数, $\max(\omega)$ 表示取集合 ω 中最大的数. $\boldsymbol{I}_3$ 与 $\boldsymbol{0}_3$ 分别表示 3×3 的单位对角阵与零矩阵. $\boldsymbol{0}_{3\times 1}$ 表示 3×1 的零矩阵.

1 四旋翼无人机模型

假设四旋翼无人机多智能体系统中具有 n 个四旋翼无人机智能体, 单个四旋翼无人机的姿态非线性动力学方程为[21]:

$$\begin{cases}I_{xi}\ddot{\phi}_i=(I_{yi}-I_{zi})\dot{\theta}_i\dot{\psi}_i+J_{ri}w_{ri}\dot{\theta}_i+u_{1i}-k_{axi}\dot{\phi}_i\\ I_{yi}\ddot{\theta}_i=(I_{zi}-I_{xi})\dot{\phi}_i\dot{\psi}_i-J_{ri}w_{ri}\dot{\phi}_i+u_{2i}-k_{ayi}\dot{\theta}_i\\ I_{zi}\ddot{\psi}_i=(I_{xi}-I_{yi})\dot{\theta}_i\dot{\phi}_i+u_{3i}-k_{azi}\dot{\psi}_i\end{cases}\tag{1}$$

其中, $i=1,\cdots,n$, ϕ_i、θ_i、ψ_i 分别表示第 i 个无人机的横滚角、俯仰角、偏航角, $\phi_i\in(-\pi/2, \pi/2)$、$\theta_i\in(-\pi/2, \pi/2)$、$\psi_i\in(0, 2\pi)$, I_{xi}, I_{yi}, I_{zi} 表示无人机体绕机体坐标系 x_b, y_b, z_b 轴的转动惯量, J_{ri} 表示无人机的电动机和桨叶的转动惯量. 输入扰动为 $w_{ri}=w_{1i}-w_{2i}+w_{3i}-w_{4i}$, 其中, $w_{1i}, w_{2i}, w_{3i}, w_{4i}$ 表示无人机四个旋翼的转速, $J_{ri}w_{ri}\dot{\theta}_i$、$J_{ri}w_{ri}\dot{\phi}_i$ 表示陀螺力矩, $k_{axi}, k_{ayi}, k_{azi}$表示空气阻力矩系数, u_{1i}, u_{2i}, u_{3i}表示无人机旋翼对其三个姿态角的控制量.

由于四旋翼无人机存在着小参量 I_{xi}, I_{yi}, I_{zi} 等, 呈现较为显著的奇异摄动现象[22]. 因此对四旋翼无人机智能体系统进行奇异摄动的建模. 定义 $\epsilon=\min(I_{xi}, I_{yi}, I_{zi})$, $\bar{I}_{xi}=I_{xi}/\epsilon$, $\bar{I}_{yi}=I_{yi}/\epsilon$, $\bar{I}_{zi}=I_{zi}/\epsilon$, $\bar{J}_{ri}=J_{ri}/\epsilon$, $\bar{k}_{axi}=k_{axi}/\epsilon$, $\bar{k}_{ayi}=k_{ayi}/\epsilon$, $\bar{k}_{azi}=k_{azi}/\epsilon$, $\hat{I}_i=\mathrm{diag}\{\bar{I}_{xi}, \bar{I}_{yi}, \bar{I}_{zi}\}$, $\boldsymbol{x}_i=(\phi_i, \theta_i, \psi_i)^{\mathrm{T}}$, $\boldsymbol{v}_i=(\dot{\phi}_i, \dot{\theta}_i, \dot{\psi}_i)^{\mathrm{T}}$, $\boldsymbol{u}_i=\hat{I}_i^{-1}(u_{1i}, u_{2i}, u_{3i})^{\mathrm{T}}$. 基于此, 第 i 个四旋翼无人机的姿态非线性动力学矩阵方程为:

$$\epsilon\ddot{\boldsymbol{x}}_i=\boldsymbol{u}_i+\boldsymbol{g}_i(\boldsymbol{v}_i, w_{ri})\tag{2}$$

其中,

$$\boldsymbol{g}_i(\boldsymbol{v}_i, w_{ri})=\begin{bmatrix}\tau_i+\dfrac{\epsilon\bar{J}_{ri}}{\bar{I}_{xi}}w_{ri}\,\dot{\theta}_i-\dfrac{\epsilon\bar{k}_{axi}}{\bar{I}_{xi}}\,\dot{\phi}_i\\ \zeta_i-\dfrac{\epsilon\bar{J}_{ri}}{\bar{I}_{yi}}w_{ri}\,\dot{\phi}_i-\dfrac{\epsilon\bar{k}_{ayi}}{\bar{I}_{yi}}\,\dot{\theta}_i\\ \dfrac{\epsilon(\bar{I}_{xi}-\bar{I}_{yi})}{\bar{I}_{zi}}\,\dot{\theta}_i\,\dot{\phi}_i-\dfrac{\epsilon\bar{k}_{azi}}{\bar{I}_{zi}}\,\dot{\psi}_i\end{bmatrix}$$

$$\tau_i(\dot{\boldsymbol{x}}_i)=\frac{\epsilon(\bar{I}_{yi}-\bar{I}_{zi})}{\bar{I}_{xi}}\,\dot{\theta}_i\,\dot{\psi}_i,\ \zeta_i(\dot{\boldsymbol{x}}_i)=\frac{\epsilon(\bar{I}_{zi}-\bar{I}_{xi})}{\bar{I}_{yi}}\,\dot{\phi}_i\,\dot{\psi}_i$$

2 系统描述与引理

将式 (2) 表示为状态空间方程:

$$\begin{cases}\dot{\boldsymbol{x}}_i(t)=\boldsymbol{v}_i(t)\\ \epsilon\dot{\boldsymbol{v}}_i(t)=\boldsymbol{u}_i(t)+\boldsymbol{g}_i(\boldsymbol{v}_i,\,w_{ri})\end{cases}\tag{3}$$

假设每个智能体都可以访问邻接的智能体的输出相对值, 并且相关的邻接矩阵表示为 $G=[a_{ij}]$, 其中 a_{ij} 表示第 i 个智能体与第 j 个智能体之间连接的权值, 若无连接则为 0, 且 $i,\,j=1,\,2,\,3,\,\cdots,\,m$.

定义一致性角度误差和角速度误差为:

$$\begin{cases}\boldsymbol{e}_{xi}(t)=\displaystyle\sum_{j=1,\,j\neq i}^{n}a_{ij}(\boldsymbol{x}_i(t)-\boldsymbol{x}_j(t))\\ \boldsymbol{e}_{vi}(t)=\displaystyle\sum_{j=1,\,j\neq i}^{n}a_{ij}(\boldsymbol{v}_i(t)-\boldsymbol{v}_j(t))\end{cases}\tag{4}$$

由式 (3)、(4), 可得以下同步误差模型:

$$\begin{cases}\dot{\boldsymbol{e}}_{xi}(t)=\boldsymbol{e}_{vi}(t)\\ \epsilon\dot{\boldsymbol{e}}_{vi}(t)=\displaystyle\sum_{j=1,\,j\neq i}^{n}a_{ij}(\boldsymbol{u}_i(t)-\boldsymbol{u}_j(t)+\\ \qquad\boldsymbol{g}_i(\boldsymbol{v}_i,\,w_{ri})-\boldsymbol{g}_j(\boldsymbol{v}_j,\,w_{rj}))\end{cases}\tag{5}$$

为了后续分析, 在此给出假设和引理.

假设 1. 令 $\bar{\boldsymbol{\varphi}}_i(t,\,\boldsymbol{g}_i)=\sum_{j=1,\,j\neq i}^{n}a_{ij}(\boldsymbol{g}_i(\boldsymbol{v}_i,\,w_{ri})-\boldsymbol{g}_j(\boldsymbol{v}_j,\,w_{rj}))$, 且 $||\bar{\boldsymbol{\varphi}}_i(t,\,\boldsymbol{g}_i)||\leq\delta_i||\boldsymbol{s}_i(t)||^{\frac{1}{2}}$, 其中, $\bar{\boldsymbol{\varphi}}_i(t,\,\boldsymbol{g}_i)$ 满足 Lipschitz 条件, $\delta_i>0$ 存在但未知.

引理 1[23]**.** 若存在矩阵 $Z_i\ (i=1,\,\cdots,\,5)$ 且 $Z_i=Z_i^{\rm T}\ (i=1,\,\cdots,\,4)$, 满足以下线性矩阵不等式:

$$Z_1>0,\ \begin{bmatrix}Z_1+\bar{\epsilon}Z_3 & \bar{\epsilon}Z_5^{\rm T}\\ \bar{\epsilon}Z_5 & \bar{\epsilon}Z_2\end{bmatrix}>0$$

则可以得到 $Z(\epsilon)>0$, 对任意的 $\epsilon\in(0,\,\bar{\epsilon}]$ 都成立, 其中, $Z(\epsilon)=\begin{bmatrix}Z_1+\epsilon Z_3 & \epsilon Z_5^{\rm T}\\ \epsilon Z_5 & \epsilon Z_2\end{bmatrix}$.

引理 2. 对于任意列向量 $\boldsymbol{z}_1$, $\boldsymbol{z}_2$ 和 $\boldsymbol{z}_3$. 有以下不等式成立:

$$\pm\boldsymbol{z}_3^{\rm T}\boldsymbol{z}_2\boldsymbol{z}_2^{\rm T}\boldsymbol{z}_1\leq||\boldsymbol{z}_2||^2||\boldsymbol{z}_1||||\boldsymbol{z}_3||$$

证明. 令 $\boldsymbol{a}=\boldsymbol{z}_2\boldsymbol{z}_2^{\rm T}\boldsymbol{z}_3$, $\boldsymbol{b}=\boldsymbol{z}_1$, 则

$$\pm\boldsymbol{a}^{\rm T}\boldsymbol{b}\leq||\boldsymbol{a}||||\boldsymbol{b}||=\sqrt{\boldsymbol{z}_3^{\rm T}\boldsymbol{z}_2\boldsymbol{z}_2^{\rm T}\boldsymbol{z}_2\boldsymbol{z}_2^{\rm T}\boldsymbol{z}_3}\cdot\sqrt{\boldsymbol{z}_1^{\rm T}\boldsymbol{z}_1}\leq\\ ||\boldsymbol{z}_2||^2||\boldsymbol{z}_1||||\boldsymbol{z}_3||$$

□

引理 3[24]**.** 给定任意正定标量 $l>0$, 对于任意标量 x, y, 有以下不等式成立: $\pm xy<lx^2+\frac{1}{4l}y^2$.

引理 4[25]**.** 对于一个 n 维非 $\boldsymbol{0}$ 列向量 $\boldsymbol{x}$, P 为 $n\times n$ 维的 Hermitian 矩阵, 有如下性质:

$$\lambda_{\min}(P)\boldsymbol{x}^{\rm T}\boldsymbol{x}\leq\boldsymbol{x}^{\rm T}P\boldsymbol{x}\leq\lambda_{\max}(P)\boldsymbol{x}^{\rm T}\boldsymbol{x}$$

3 四旋翼无人机集群姿态角一致性分析

设计以下受导引型奇异摄动二阶滑模动态:

$$\boldsymbol{s}_i(t)=\boldsymbol{e}_{xi}(t)+\epsilon\boldsymbol{e}_{vi}(t)+l_i(\boldsymbol{x}_1(t)-\boldsymbol{x}_0(t))\tag{6}$$

其中, l_i 表示追踪系数, $l_1>0$, $l_i=0\ (i\neq1)$, $\boldsymbol{x}_0(t)$ 表示姿态角的跟踪值, $\boldsymbol{s}_i(t)$ 表示第 i 个滑模变量.

根据式 (5) 可得, 滑模动态 (6) 的一阶导数为:

$$\dot{\boldsymbol{s}}_i(t)=\boldsymbol{e}_{vi}(t)+\sum_{j=1,\,j\neq i}^{n}a_{ij}(\boldsymbol{u}_i(t)-\boldsymbol{u}_j(t)+\\ \boldsymbol{g}_i(\boldsymbol{v}_i,\,w_{ri})-\boldsymbol{g}_j(\boldsymbol{v}_j,\,w_{rj}))+\\ l_i(\dot{\boldsymbol{x}}_1(t)-\dot{\boldsymbol{x}}_0(t))\tag{7}$$

3.1 自适应多尺度超螺旋算法

受文献 [26] 的启发, 考虑到系统 (5) 的两时间尺度特性, 设计以下自适应 STW 滑模控制器:

$$\begin{cases}\boldsymbol{u}_i(t)=\left(\displaystyle\sum_{j=1,\,j\neq i}^{n}a_{ij}\right)^{-1}\left(-\alpha_i(t)\frac{\boldsymbol{s}_i(t)}{||\boldsymbol{s}_i(t)||^{\frac{1}{2}}}+\boldsymbol{r}_i(t)-\right.\\ \qquad\displaystyle\sum_{j=1,\,j\neq i}^{n}a_{ij}(\boldsymbol{v}_i(t)-\boldsymbol{v}_j(t))+\\ \qquad\left.\displaystyle\sum_{j=1,\,j\neq i}^{n}a_{ij}\boldsymbol{u}_j(t)-l_i(\dot{\boldsymbol{x}}_1(t)-\dot{\boldsymbol{x}}_0(t))\right)\\ \epsilon\dot{\boldsymbol{r}}_i(t)=-\beta_i(t)\dfrac{\boldsymbol{s}_i(t)}{||\boldsymbol{s}_i(t)||}\end{cases}\tag{8}$$

其中, $\alpha_i(t)$ 和 $\beta_i(t)$ 表示两个自适应增益.

将式 (8) 代入式 (7), 可得:

$$\begin{cases}\dot{\boldsymbol{s}}_i(t)=\displaystyle\sum_{j=1,\,j\neq i}^{n}a_{ij}(\boldsymbol{g}_i(\boldsymbol{v}_i,\,w_{ri})-\boldsymbol{g}_j(\boldsymbol{v}_j,\,w_{rj}))-\\ \qquad\alpha_i(t)\dfrac{\boldsymbol{s}_i(t)}{||\boldsymbol{s}_i(t)||^{\frac{1}{2}}}+\boldsymbol{r}_i(t)\\ \epsilon\dot{\boldsymbol{r}}_i(t)=-\beta_i(t)\dfrac{\boldsymbol{s}_i(t)}{||\boldsymbol{s}_i(t)||}\end{cases}\tag{9}$$

下面的定理研究了在自适应多尺度 STW 算法控制下的四旋翼无人机群在有限时间内的姿态协同.

定理 1. 给定 $p_{1i}>0$, $p_{2i}>0$, $b_{1i}>0$, $b_{2i}>0$, $\gamma_{1i}>0$, $\gamma_{2i}>0$, 存在 $\bar{\epsilon}>0$, 当满足:

$$\begin{bmatrix}p_{1i}\boldsymbol{I}_3 & \bar{\epsilon}p_{2i}\boldsymbol{I}_3\\ \bar{\epsilon}p_{2i}\boldsymbol{I}_3 & \bar{\epsilon}p_{3i}\boldsymbol{I}_3\end{bmatrix}>0\tag{10}$$

以及系统的自适应增益导数满足:

$$\dot{\alpha}_i(t)=b_{1i}\sqrt{\frac{\gamma_{1i}}{2}},\quad \dot{\beta}_i(t)=b_{2i}\sqrt{\frac{\gamma_{2i}}{2}} \tag{11}$$

则对任意的 $\epsilon\in(0,\bar{\epsilon}]$, 四旋翼无人机集群系统的姿态角将会在有限时间内趋于一致.

证明. 构造新的状态变量:

$$\begin{cases}\boldsymbol{z}_i=\text{col}\{\boldsymbol{z}_{1i},\,\boldsymbol{z}_{2i}\}\\ \boldsymbol{z}_{1i}=\text{diag}\{\text{sgn}(\boldsymbol{s}_i(t))\}\dfrac{\boldsymbol{s}_i(t)}{||\boldsymbol{s}_i(t)||^{\frac{1}{2}}}\\ \boldsymbol{z}_{2i}=\text{diag}\{\text{sgn}(\boldsymbol{s}_i(t))\}\boldsymbol{r}_i(t)\end{cases} \tag{12}$$

根据式 (9)、(12), 可得:

$$\begin{bmatrix}\dot{\boldsymbol{z}}_{1i}\\ \epsilon\dot{\boldsymbol{z}}_{2i}\end{bmatrix}=\frac{1}{||\boldsymbol{z}_{1i}||}\begin{bmatrix}-\frac{1}{2}\alpha_i(t)\boldsymbol{I}_3 & \boldsymbol{I}_3\\ -\beta_i(t)\boldsymbol{I}_3 & \boldsymbol{0}_3\end{bmatrix}\begin{bmatrix}\boldsymbol{z}_{1i}\\ \boldsymbol{z}_{2i}\end{bmatrix}+\frac{1}{||\boldsymbol{z}_{1i}||}\begin{bmatrix}\boldsymbol{\varphi}_i(t,\,\boldsymbol{g}_i)\\ \boldsymbol{0}_{3\times1}\end{bmatrix}+\boldsymbol{\eta}_i \tag{13}$$

其中, $\boldsymbol{\eta}_i=\text{col}\{-\frac{\boldsymbol{z}_{1i}\boldsymbol{z}_{1i}^{\mathrm{T}}}{2||\boldsymbol{z}_{1i}||^3}(\boldsymbol{z}_{2i}+\boldsymbol{\varphi}_i(t,\,\boldsymbol{g}_i)),\,\boldsymbol{0}_{3\times1}\}$, $\boldsymbol{\varphi}_i(t,\,\boldsymbol{g}_i)=\text{diag}\{\text{sgn}(\boldsymbol{s}_i(t))\}\bar{\boldsymbol{\varphi}}_i(t,\,\boldsymbol{g}_i)$.

由式 (11)、(13), 可知: 当 $\boldsymbol{z}_{1i}$, $\boldsymbol{z}_{2i}$ 趋于 $\boldsymbol{0}$ 时, $\boldsymbol{s}_i$ 会趋于 $\boldsymbol{0}$, 再根据式 (9) 以及假设 1, $\dot{\boldsymbol{s}}_i$ 也会趋于 $\boldsymbol{0}$.

考虑以下奇异摄动 Lyapunov 函数:

$$V(t,\,\epsilon)=\sum_{i=1}^{m}V_i(t,\,\epsilon),\ P_i(\epsilon)=(\bar{P}_i(\epsilon)F_\epsilon)\otimes\boldsymbol{I}_3$$

$$V_i(t,\,\epsilon):=\boldsymbol{z}_i^{\mathrm{T}}P_i(\epsilon)\boldsymbol{z}_i+\frac{1}{2\gamma_{1i}}(\alpha_i(t)-\hat{\alpha}_i)^2+\frac{1}{2\gamma_{2i}}(\beta_i(t)-\hat{\beta}_i)^2$$

其中, $F_\epsilon=\text{diag}\{1,\,\epsilon\}$

$$\bar{P}_i(\epsilon)=\begin{bmatrix}p_{1i} & p_{2i}\\ \epsilon p_{2i} & p_{3i}\end{bmatrix}$$

$\hat{\alpha}_i$ 表示 $\alpha_i(t)$ 的上界, $\hat{\beta}_i$ 表示 $\beta_i(t)$ 的上界. 根据引理 1, $P_i(\epsilon)>0$ 成立的充分条件为式 (10). 定义 $V_{0i}(t,\,\epsilon)=\boldsymbol{z}_i^{\mathrm{T}}P_i(\epsilon)\boldsymbol{z}_i$, 并对其求导可得:

$$\dot{V}_{0i}(t,\,\epsilon)=-\frac{1}{||\boldsymbol{z}_{1i}||}\boldsymbol{z}_i^{\mathrm{T}}\bar{Q}_i(\epsilon)\boldsymbol{z}_i+2\boldsymbol{z}_i^{\mathrm{T}}\bar{P}_i(\epsilon)\boldsymbol{\eta}_i+\frac{1}{||\boldsymbol{z}_{1i}||}2\boldsymbol{z}_i^{\mathrm{T}}(\Omega_{0i}(\epsilon)\otimes\boldsymbol{I}_3)\boldsymbol{\varphi}_i(t,\,\boldsymbol{g}_i) \tag{14}$$

其中,

$$\Omega_{0i}(\epsilon)=\begin{bmatrix}p_{1i}\\ \epsilon p_{2i}\end{bmatrix},\ \bar{Q}_i(\epsilon)=\begin{bmatrix}q_{11} & *\\ q_{12} & 2\epsilon p_{2i}\end{bmatrix}\otimes\boldsymbol{I}_3$$

$$q_{11}=\alpha_i(t)p_{1i}+2\epsilon\beta_i(t)p_{2i}$$

$$q_{12}=\frac{1}{2}\alpha_i(t)p_{2i}\epsilon+\beta_i(t)p_{3i}-p_{1i}$$

由假设 1, 可知:

$$|\boldsymbol{\varphi}_i(t,\,\boldsymbol{g}_i)|\le\delta_i|\boldsymbol{z}_{1i}|=[\delta_i\quad 0]\otimes\boldsymbol{I}_3\boldsymbol{z}_i$$

可以构造以下不等式:

$$2\boldsymbol{z}_i^{\mathrm{T}}(\Omega_{0i}(\epsilon)\otimes\boldsymbol{I}_3)\boldsymbol{\varphi}_i(t,\,\boldsymbol{g}_i)\le\boldsymbol{z}_i^{\mathrm{T}}(\Lambda(\epsilon)\otimes\boldsymbol{I}_3)\boldsymbol{z}_i \tag{15}$$

其中,

$$\Lambda(\epsilon)=\begin{bmatrix}2p_{1i}\delta_i & *\\ \epsilon p_{2i}\delta_i & 0\end{bmatrix}$$

令 $p(t)=2\boldsymbol{z}_i^{\mathrm{T}}\bar{P}_i(\epsilon)\boldsymbol{\eta}_i$, 易得:

$$p(t)=-\frac{p_{1i}\boldsymbol{z}_{1i}^{\mathrm{T}}\boldsymbol{z}_{1i}\boldsymbol{z}_{1i}^{\mathrm{T}}\boldsymbol{z}_{2i}}{||\boldsymbol{z}_{1i}||^3}-\frac{\epsilon p_{2i}\boldsymbol{z}_{2i}^{\mathrm{T}}\boldsymbol{z}_{1i}\boldsymbol{z}_{1i}^{\mathrm{T}}\boldsymbol{\varphi}_i(t,\,\boldsymbol{g}_i)}{||\boldsymbol{z}_{1i}||^3}-\frac{p_{1i}\boldsymbol{z}_{1i}^{\mathrm{T}}\boldsymbol{z}_{1i}\boldsymbol{z}_{1i}^{\mathrm{T}}\boldsymbol{\varphi}_i(t,\,\boldsymbol{g}_i)}{||\boldsymbol{z}_{1i}||^3}-\frac{\epsilon p_{2i}\boldsymbol{z}_{2i}^{\mathrm{T}}\boldsymbol{z}_{1i}\boldsymbol{z}_{1i}^{\mathrm{T}}\boldsymbol{z}_{2i}}{||\boldsymbol{z}_{1i}||^3} \tag{16}$$

由引理 2, 将式 (16) 转化为:

$$p(t)\le\frac{p_{1i}}{||\boldsymbol{z}_{1i}||}(||\boldsymbol{z}_{1i}||\cdot||\boldsymbol{z}_{2i}||+||\boldsymbol{z}_{1i}||\cdot||\boldsymbol{\varphi}_i(t,\,\boldsymbol{g}_i)||)-\frac{\epsilon p_{2i}}{||\boldsymbol{z}_{1i}||}(||\boldsymbol{z}_{2i}||\cdot||\boldsymbol{z}_{2i}||+||\boldsymbol{z}_{2i}||\cdot||\boldsymbol{\varphi}_i(t,\,\boldsymbol{g}_i)||) \tag{17}$$

由引理 3, 可构造:

$$\begin{cases}||\boldsymbol{z}_{1i}||\cdot||\boldsymbol{z}_{2i}||\le c_{1i}\boldsymbol{z}_{1i}^{\mathrm{T}}\boldsymbol{z}_{1i}+\dfrac{1}{4c_{1i}}\boldsymbol{z}_{2i}^{\mathrm{T}}\boldsymbol{z}_{2i}\\ ||\boldsymbol{z}_{1i}||\cdot||\boldsymbol{\varphi}_i||\le c_{2i}\boldsymbol{z}_{1i}^{\mathrm{T}}\boldsymbol{z}_{1i}+\dfrac{1}{4c_{2i}}\boldsymbol{\varphi}_i^{\mathrm{T}}\boldsymbol{\varphi}_i\\ ||\boldsymbol{z}_{2i}||\cdot||\boldsymbol{\varphi}_i||\le c_{3i}\boldsymbol{z}_{2i}^{\mathrm{T}}\boldsymbol{z}_{2i}+\dfrac{1}{4c_{3i}}\boldsymbol{\varphi}_i^{\mathrm{T}}\boldsymbol{\varphi}_i\end{cases} \tag{18}$$

联立式 (17) 和式 (18), 可得:

$$p(t)\le\frac{1}{||\boldsymbol{z}_{1i}||}\boldsymbol{z}_i^{\mathrm{T}}(Y_i(\epsilon)\otimes\boldsymbol{I}_3)\boldsymbol{z}_i \tag{19}$$

其中, $Y_i(\epsilon)=\text{diag}\{d_1,\,d_2\}$

$$d_1=p_{1i}\left(c_{1i}+c_{2i}+\frac{\delta_1^2}{4c_{2i}}\right)-\frac{\epsilon p_{2i}\delta_1^2}{4c_{3i}}$$

$$d_2=\frac{\delta_1^2}{4c_{1i}}-\epsilon p_{2i}(1+c_{3i})$$

联立式 (14)、(15)、(19), 可得:

$$\dot{V}_{0i}(t,\,\epsilon)\le-\boldsymbol{z}_i^{\mathrm{T}}Q_i(\epsilon)\boldsymbol{z}_i \tag{20}$$

其中,

$$Q_i(\epsilon)=\begin{bmatrix}\bar{q}_1 & *\\ \bar{q}_2 & \bar{q}_3\end{bmatrix}\otimes\boldsymbol{I}_3,$$

$$\bar{q}_1=\alpha_i(t)p_{1i}+2\epsilon\beta_i(t)p_{2i}-2p_{1i}\delta_1-d_1$$

$$\bar{q}_2=\frac{1}{2}\alpha_i(t)p_{2i}\epsilon+\beta_i(t)p_{3i}-p_{1i}-\epsilon p_{2i}\delta_i$$

$$\bar{q}_3=2\epsilon p_{2i}-d_2$$

设计 $\beta_i(t)=-\frac{\epsilon p_{2i}}{2p_{3i}}\alpha_i(t)+\frac{p_{1i}}{p_{3i}}$. 根据 Schur 补引理[27], 可得 $Q_i(\epsilon)>0$, 当以下条件成立时:

$$\alpha_i(t)>\frac{\epsilon^2p_{2i}^2\delta_i^2p_{3i}+\bar{q}_3p_{3i}(d_1+2p_{1i}\delta_i)}{\bar{q}_3(p_{3i}p_{1i}+2\epsilon p_{1i}-\epsilon^2p_{2i})}$$

由引理 4, 可知:

$$\begin{cases}\lambda_{\min}(Q_i)||\boldsymbol{z}_i||^2\le\boldsymbol{z}_i^{\mathrm{T}}Q_i(\epsilon)\boldsymbol{z}_i\le\lambda_{\max}(Q_i)||\boldsymbol{z}_i||^2\\\lambda_{\min}(P_i)||\boldsymbol{z}_i||^2\le\boldsymbol{z}_i^{\mathrm{T}}P_i(\epsilon)\boldsymbol{z}_i\le\lambda_{\max}(P_i)||\boldsymbol{z}_i||^2\end{cases}\tag{21}$$

基于式 (21), 我们有:

$$||\boldsymbol{z}_{1i}||\le||\boldsymbol{z}_i||\le\frac{(\boldsymbol{z}_i^{\mathrm{T}}P_i(\epsilon)\boldsymbol{z}_i)^{\frac{1}{2}}}{\lambda_{\min}^{\frac{1}{2}}(P_i)},\ ||\boldsymbol{z}_i||^2\ge\frac{\boldsymbol{z}_i^{\mathrm{T}}P_i(\epsilon)\boldsymbol{z}_i}{\lambda_{\max}(P_i)}\tag{22}$$

根据式 (20)、(21)、(22), 可得:

$$\dot{V}_{0i}(t,\epsilon)\le-\frac{1}{||\boldsymbol{z}_{1i}||}\lambda_{\min}(Q_i)||\boldsymbol{z}_i||^2\le-r_{1i}V_{0i}^{\frac{1}{2}}(t,\epsilon)\tag{23}$$

其中, $r_{1i}=\frac{\lambda_{\min}(Q_i)\lambda_{\min}^{\frac{1}{2}}(P_i)}{\lambda_{\max}(P_i)}$.

由于 $\beta_i(t)\le\hat{\beta}_i$, $\alpha_i(t)\le\hat{\alpha}_i$. 结合式 (23), 可得:

$$\begin{aligned}\dot{V}_i(t,\epsilon)\le&-r_{1i}V_{0i}^{\frac{1}{2}}(t,\epsilon)-\frac{b_{1i}}{\sqrt{2\gamma_{1i}}}|\alpha_i(t)-\hat{\alpha}_i|-\\&\frac{b_{2i}}{\sqrt{2\gamma_{2i}}}\cdot|\beta_i(t)-\hat{\beta}_i|-|\alpha_i(t)-\\&\hat{\alpha}_i|\left(\frac{1}{\gamma_{1i}}\dot{\alpha}_i(t)-\frac{b_{1i}}{\sqrt{2\gamma_{1i}}}\right)-\\&|\beta_i(t)-\hat{\beta}_i|\left(\frac{1}{\gamma_{2i}}\dot{\beta}_i(t)-\frac{b_{2i}}{\sqrt{2\gamma_{2i}}}\right)\end{aligned}\tag{24}$$

令式 (24) 中 $\frac{1}{\gamma_{1i}}\dot{\alpha}_i(t)-\frac{b_{1i}}{\sqrt{2\gamma_{1i}}}=0$, $\frac{1}{\gamma_{2i}}\dot{\beta}_i(t)-\frac{b_{2i}}{\sqrt{2\gamma_{2i}}}=0$, 则可得 $\alpha_i(t)$, $\beta_i(t)$ 应满足式 (11). 将式 (11) 代入式 (24) 中, 根据柯西不等式[28], 可得:

$$\begin{aligned}\dot{V}(t,\epsilon)=&\sum_{i=1}^{m}\dot{V}_i(t,\epsilon)\le-\sum_{i=1}^{m}\check{r}_iV_i^{\frac{1}{2}}(t,\epsilon)\le\\&-\check{r}_k\left(\sum_{i=1}^{m}V(t,\epsilon)\right)^{\frac{1}{2}}\le-\check{r}_kV^{\frac{1}{2}}(t,\epsilon)\end{aligned}\tag{25}$$

其中, $\check{r}_i=\min(r_{1i},b_{1i},b_{2i})$, $\check{r}_k=\min(\check{r}_i)$.

由此可见, 四旋翼无人机集群系统的一致性误差在有限时间内稳定. □

3.2 改进型自适应多尺度超螺旋算法

由于定理 1 中, 在自适应多尺度 STW 算法控制下的系统收敛时间相对较长. 因此在文献 [29] 的启发下, 设计以下改进型自适应 STW 滑模控制器:

$$\begin{cases}\boldsymbol{u}_i(t)=\left(\sum\limits_{j=1,\,j\ne i}^{n}a_{ij}\right)^{-1}\Bigg(-\alpha_i(t)\dfrac{\boldsymbol{s}_i(t)}{||\boldsymbol{s}_i(t)||^{\frac{1}{2}}}+\boldsymbol{r}_i(t)-\\\qquad\sum\limits_{j=1,\,j\ne i}^{n}a_{ij}(\boldsymbol{v}_i(t)-\boldsymbol{v}_j(t))-k_{1i}\boldsymbol{s}_i(t)+\\\qquad\sum\limits_{j=1,\,j\ne i}^{n}a_{ij}\boldsymbol{u}_j(t)-l_i(\dot{\boldsymbol{x}}_1(t)-\dot{\boldsymbol{x}}_0(t))\Bigg)\\\epsilon\dot{\boldsymbol{r}}_i(t)=-\beta_i(t)\dfrac{\boldsymbol{s}_i(t)}{||\boldsymbol{s}_i(t)||}-k_{2i}\boldsymbol{s}_i(t)\end{cases}\tag{26}$$

其中, k_{1i}、k_{2i} 为两个增益.

将式 (26) 代入式 (6), 可得:

$$\begin{cases}\dot{\boldsymbol{s}}_i(t)=-\alpha_i(t)\dfrac{\boldsymbol{s}_i(t)}{||\boldsymbol{s}_i(t)||^{\frac{1}{2}}}+\boldsymbol{r}_i(t)-k_{1i}\boldsymbol{s}_i(t)+\\\qquad\bar{\boldsymbol{\varphi}}_i(t,\boldsymbol{g}_i)\\\epsilon\dot{\boldsymbol{r}}_i(t)=-\beta_i(t)\dfrac{\boldsymbol{s}_i(t)}{||\boldsymbol{s}_i(t)||}-k_{2i}\boldsymbol{s}_i(t)\end{cases}\tag{27}$$

下面的定理研究了在改进型自适应多尺度 STW 滑模算法的控制下, 四旋翼无人机集群系统的姿态角能够快速地趋于一致.

定理 2. 给定 $b_{3i}>0$, $b_{4i}>0$, $b_{5i}>\hat{\alpha}_i$, $b_{6i}>\hat{\beta}_i$. 在控制器 (26) 作用下, 系统状态将快速趋于一致, 当存在 $\bar{\epsilon}>0$, 使得以下式子成立时:

$$W_i(\bar{\epsilon})>0,\ P_{2i}(\bar{\epsilon})>0,\ X_i(\bar{\epsilon})>0\tag{28}$$

其中,

$$W_i(\bar{\epsilon})=\begin{bmatrix}w_{11}+\bar{\epsilon}\tilde{w}_{11}&*&*\\w_{21}&w_{22}&*\\w_{31}+\bar{\epsilon}\tilde{w}_{31}&w_{32}+\bar{\epsilon}\tilde{w}_{32}&w_{33}+\bar{\epsilon}\tilde{w}_{33}\end{bmatrix}$$

$$P_{2i}(\bar{\epsilon})=\begin{bmatrix}p_{11i}&*&*\\p_{12i}&p_{22i}&*\\\bar{\epsilon}p_{13i}&\bar{\epsilon}p_{23i}&\bar{\epsilon}p_{33i}\end{bmatrix}$$

$$X_i(\bar{\epsilon})=\begin{bmatrix}x_{11}&*&*\\x_{21}&x_{22}&*\\x_{31}+\bar{\epsilon}\tilde{x}_{31}&x_{32}+\bar{\epsilon}\tilde{x}_{32}&\bar{\epsilon}\tilde{x}_{33}\end{bmatrix}$$

对应的相关参数为:

$$\begin{aligned}w_{11}=&(\alpha_i(t)-2\delta_i-c_{4i}-c_{5i})p_{11i}+\\&2\beta_i(t)p_{13i}-\left(\frac{p_{11i}}{4c_{5i}}+\frac{p_{12i}}{4c_{7i}}\right)\delta_i^2\end{aligned}$$

$$w_{21}=\frac{1}{2}\left(\alpha_i(t)-\delta_i\right)p_{12i}+\beta_i(t)p_{23i}+\frac{1}{2}k_{1i}p_{11i}$$

$$w_{31}=\beta_i(t)p_{33i}-p_{11i},\ \tilde{w}_{31}=\frac{1}{2}(\alpha_i(t)-\delta_i)p_{13i}$$

$w_{22} = (k_{1i} - c_{6i} - c_{7i})p_{12i}$, $\tilde{w}_{33} = -(1 - c_{8i})p_{13i}$

$w_{32} = -p_{12i}$, $\tilde{w}_{32} = -\frac{1}{2}k_{1i}p_{13i}$, $\tilde{w}_{11} = \frac{p_{13i}}{4c_{8i}}\delta_i^2$

$x_{11} = 2(\alpha_i(t) - \delta_i)p_{12i}$, $x_{22} = 2k_{1i}p_{22i} + 2k_{2i}p_{23i}$

$x_{21} = (\alpha_i(t) - \delta_i)p_{22i} + k_{1i}p_{12i} + k_{2i}p_{13i}$

$x_{31} = -p_{12i}$, $\tilde{x}_{31} = (\alpha_i(t) - \delta_i)p_{23i}$

$x_{23} = k_{2i}p_{33i} - p_{22i}$, $\tilde{x}_{23} = k_{1i}p_{23i}$, $\tilde{x}_{33} = -2p_{23i}$

$\dot{\alpha}_i(t) = b_{1i}\sqrt{\frac{\gamma_{1i}}{2}} + \frac{b_{3i}b_{5i}}{2}$, $\dot{\beta}_i(t) = b_{2i}\sqrt{\frac{\gamma_{2i}}{2}} + \frac{b_{4i}b_{6i}}{2}$

证明. 构造新的状态变量:

$$\begin{cases}\hat{\boldsymbol{z}}_i = \mathrm{col}\{\hat{\boldsymbol{z}}_{1i}, \hat{\boldsymbol{z}}_{2i}, \hat{\boldsymbol{z}}_{3i}\}\\ \hat{\boldsymbol{z}}_{1i} = \mathrm{diag}\{\mathrm{sgn}(\boldsymbol{s}_i(t))\}\dfrac{\boldsymbol{s}_i(t)}{||\boldsymbol{s}_i(t)||^{\frac{1}{2}}}\\ \hat{\boldsymbol{z}}_{2i} = \mathrm{diag}\{\mathrm{sgn}(\boldsymbol{s}_i(t))\}\boldsymbol{s}_i(t)\\ \hat{\boldsymbol{z}}_{3i} = \mathrm{diag}\{\mathrm{sgn}(\boldsymbol{s}_i(t))\}\boldsymbol{r}_i(t)\end{cases} \tag{29}$$

根据式 (27)、(29), 可得:

$$E_\epsilon\dot{\hat{\boldsymbol{z}}}_i = \frac{1}{||\hat{\boldsymbol{z}}_{1i}||}(A_0\hat{\boldsymbol{z}}_i + B_0\boldsymbol{\varphi}_i(t, \boldsymbol{g}_i)) + A_1\hat{\boldsymbol{z}}_i + B_1\boldsymbol{\varphi}_i(t, \boldsymbol{g}_i) + \boldsymbol{\eta}_{2i}$$

其中, $E_\epsilon = \mathrm{diag}\{\boldsymbol{I}_3, \boldsymbol{I}_3, \epsilon\boldsymbol{I}_3\}$

$$A_0 = \begin{bmatrix} -\frac{1}{2}\alpha_i(t)\boldsymbol{I}_3 & -\frac{1}{2}k_{1i}\boldsymbol{I}_3 & \boldsymbol{I}_3\\ \boldsymbol{0}_3 & \boldsymbol{0}_3 & \boldsymbol{0}_3\\ -\beta_i(t)\boldsymbol{I}_3 & \boldsymbol{0}_3 & \boldsymbol{0}_3\end{bmatrix}, B_0 = \begin{bmatrix}\boldsymbol{I}_3\\ \boldsymbol{0}_3\\ \boldsymbol{0}_3\end{bmatrix}$$

$$A_1 = \begin{bmatrix} \boldsymbol{0}_3 & \boldsymbol{0}_3 & \boldsymbol{0}_3\\ -\alpha_i(t)\boldsymbol{I}_3 & -k_{1i}\boldsymbol{I}_3 & \boldsymbol{I}_3\\ \boldsymbol{0}_3 & -k_{2i}\boldsymbol{I}_3 & \boldsymbol{0}_3\end{bmatrix}, B_1 = \begin{bmatrix}\boldsymbol{0}_3\\ \boldsymbol{I}_3\\ \boldsymbol{0}_3\end{bmatrix}$$

$$\boldsymbol{\eta}_{2i} = \mathrm{col}\left\{-\frac{\hat{\boldsymbol{z}}_{2i}\hat{\boldsymbol{z}}_{2i}^{\mathrm{T}}}{2||\hat{\boldsymbol{z}}_{1i}||^5}(\hat{\boldsymbol{z}}_{3i} + \boldsymbol{\varphi}_i(t, \boldsymbol{g}_i)), \boldsymbol{0}_{3\times 1}, \boldsymbol{0}_{3\times 1}\right\}$$

考虑以下奇异摄动 Lyapunov 函数:

$$\bar{V}(t, \epsilon) = \sum_{i=1}^{m} V_{2i}(t, \epsilon)$$

$$V_{2i}(t, \epsilon) := \hat{\boldsymbol{z}}_i^{\mathrm{T}}P_{2i}(\epsilon)\hat{\boldsymbol{z}}_i + \frac{1}{2\gamma_{1i}}(\alpha_i(t) - \hat{\alpha}_i)^2 + \frac{1}{2\gamma_{2i}}(\beta_i(t) - \hat{\beta}_i)^2 \tag{30}$$

其中, $P_{2i}(\epsilon) = (\bar{P}_{2i}(\epsilon)E_\epsilon)\otimes\boldsymbol{I}_3 > 0$,

$$\bar{P}_{2i}(\epsilon) = \begin{bmatrix} p_{11i} & p_{12i} & p_{13i}\\ p_{12i} & p_{22i} & p_{23i}\\ \epsilon p_{13i} & \epsilon p_{23i} & p_{33i}\end{bmatrix}$$

定义 $V_{20i}(t, \epsilon) = \hat{\boldsymbol{z}}_i^{\mathrm{T}}P_{2i}(\epsilon)\hat{\boldsymbol{z}}_i$, 对其求导可得:

$$\begin{aligned}\dot{V}_{20i}(t, \epsilon) = &-\frac{1}{||\hat{\boldsymbol{z}}_{1i}||}\hat{\boldsymbol{z}}_i^{\mathrm{T}}(\Omega_{1i}(\epsilon)\otimes\boldsymbol{I}_3)\hat{\boldsymbol{z}}_i - \\ &\hat{\boldsymbol{z}}_i^{\mathrm{T}}(\Omega_{2i}(\epsilon)\otimes\boldsymbol{I}_3)\hat{\boldsymbol{z}}_i + 2\hat{\boldsymbol{z}}_i^{\mathrm{T}}\bar{P}_{2i}(\epsilon)\boldsymbol{\eta}_{2i} + \\ &\frac{1}{||\hat{\boldsymbol{z}}_{1i}||}(2\hat{\boldsymbol{z}}_i^{\mathrm{T}}(\Omega_{3i}(\epsilon)\otimes\boldsymbol{I}_3)\varphi_i(t, \boldsymbol{g}_i) + \\ &2\hat{\boldsymbol{z}}_i^{\mathrm{T}}(\Omega_{4i}(\epsilon)\otimes\boldsymbol{I}_3)\varphi_i(t, \boldsymbol{g}_i)\end{aligned} \tag{31}$$

其中,

$$\Omega_{1i}(\epsilon) = \begin{bmatrix} q_{11} & q_{12} & q_{13}\\ * & k_{1i}p_{12i} & q_{23}\\ * & * & -2\epsilon p_{13i}\end{bmatrix}$$

$$\Omega_{2i}(\epsilon) = \begin{bmatrix} 2\alpha_i(t)p_{12i} & \bar{q}_{12} & \bar{q}_{13}\\ * & \bar{q}_{22} & \bar{q}_{23}\\ * & * & -2\epsilon p_{23i}\end{bmatrix}$$

$$\Omega_{3i}(\epsilon) = \begin{bmatrix} p_{11i}\\ p_{12i}\\ \epsilon p_{13i}\end{bmatrix}$$

$$\Omega_{4i}(\epsilon) = \begin{bmatrix} p_{12i}\\ p_{22i}\\ \epsilon p_{23i}\end{bmatrix}$$

对应的相关参数为:

$$q_{11} = \alpha_i p_{11i} + 2\beta_i p_{13i}$$

$$q_{12} = \frac{1}{2}\alpha_i p_{12i} + 2\beta_i p_{23i} + \frac{1}{2}k_{1i}p_{11i}$$

$$q_{13} = \frac{1}{2}\epsilon\alpha_i p_{13i} + 2\beta_i p_{33i} - p_{11i}$$

$$q_{23} = \frac{1}{2}\epsilon k_{1i}p_{13i} - p_{12i}$$

$$\bar{q}_{12} = \alpha_i p_{22i} + k_{1i}p_{12i} + k_{2i}p_{13i}$$

$$\bar{q}_{13} = \epsilon\alpha_i p_{23i} - p_{12i}$$

$$\bar{q}_{22} = 2k_{1i}p_{22i} + 2k_{2i}p_{23i}$$

$$\bar{q}_{23} = \epsilon k_{1i}p_{23i} + k_{2i}p_{33i} - p_{22i}$$

由假设 1, 可知:

$$|\boldsymbol{\varphi}_i(t, \boldsymbol{g}_i)| \le \delta_i|\hat{\boldsymbol{z}}_{1i}| = [\delta_i \quad 0 \quad 0]\otimes\boldsymbol{I}_3\hat{\boldsymbol{z}}_i$$

可以构造以下不等式:

$$\begin{cases}2\hat{\boldsymbol{z}}_i^{\mathrm{T}}(\Omega_{3i}(\epsilon)\otimes\boldsymbol{I}_3)\boldsymbol{\varphi}_i(t, \boldsymbol{g}_i) \le \hat{\boldsymbol{z}}_i^{\mathrm{T}}(\Lambda_0(\epsilon)\otimes\boldsymbol{I}_3)\hat{\boldsymbol{z}}_i\\ 2\hat{\boldsymbol{z}}_i^{\mathrm{T}}(\Omega_{4i}(\epsilon)\otimes\boldsymbol{I}_3)\boldsymbol{\varphi}_i(t, \boldsymbol{g}_i) \le \hat{\boldsymbol{z}}_i^{\mathrm{T}}(\Lambda_1(\epsilon)\otimes\boldsymbol{I}_3)\hat{\boldsymbol{z}}_i\end{cases} \tag{32}$$

其中,

$$\Lambda_0(\epsilon) = \begin{bmatrix} 2\delta_i p_{11i} & \delta_i p_{12i} & \epsilon\delta_i p_{13i}\\ * & 0 & 0\\ * & * & 0\end{bmatrix}$$

$$\Lambda_1(\epsilon)=\begin{bmatrix}2\delta_i p_{12i} & \delta_i p_{22i} & \epsilon\delta_i p_{23i}\\ * & 0 & 0\\ * & * & 0\end{bmatrix}$$

令 $p_2(t)=2\hat{\boldsymbol{z}}_i^{\mathrm{T}}\bar{P}_{2i}(\epsilon)\boldsymbol{\eta}_{2i}$, 易得:

$$\begin{aligned}p_2(t)=&-\frac{p_{11i}\hat{\boldsymbol{z}}_{1i}^{\mathrm{T}}\hat{\boldsymbol{z}}_{2i}\hat{\boldsymbol{z}}_{2i}^{\mathrm{T}}\hat{\boldsymbol{z}}_{3i}}{||\hat{\boldsymbol{z}}_{1i}||^5}-\frac{\epsilon p_{13i}\hat{\boldsymbol{z}}_{3i}^{\mathrm{T}}\hat{\boldsymbol{z}}_{2i}\hat{\boldsymbol{z}}_{2i}^{\mathrm{T}}\boldsymbol{\varphi}_i(t,\boldsymbol{g}_i)}{||\hat{\boldsymbol{z}}_{1i}||^5}-\\&\frac{\epsilon p_{13i}\hat{\boldsymbol{z}}_{3i}^{\mathrm{T}}\hat{\boldsymbol{z}}_{2i}\hat{\boldsymbol{z}}_{2i}^{\mathrm{T}}\hat{\boldsymbol{z}}_{3i}}{||\hat{\boldsymbol{z}}_{1i}||^5}-\frac{p_{11i}\hat{\boldsymbol{z}}_{1i}^{\mathrm{T}}\hat{\boldsymbol{z}}_{2i}\hat{\boldsymbol{z}}_{2i}^{\mathrm{T}}\boldsymbol{\varphi}_i(t,\boldsymbol{g}_i)}{||\hat{\boldsymbol{z}}_{1i}||^5}-\\&\frac{p_{12i}\hat{\boldsymbol{z}}_{2i}^{\mathrm{T}}\hat{\boldsymbol{z}}_{2i}\hat{\boldsymbol{z}}_{2i}^{\mathrm{T}}\boldsymbol{\varphi}_i(t,\boldsymbol{g}_i)}{||\hat{\boldsymbol{z}}_{1i}||^5}-\frac{p_{12i}\hat{\boldsymbol{z}}_{2i}^{\mathrm{T}}\hat{\boldsymbol{z}}_{2i}\hat{\boldsymbol{z}}_{2i}^{\mathrm{T}}\boldsymbol{z}_{3i}}{||\hat{\boldsymbol{z}}_{1i}||^5}\end{aligned}\tag{33}$$

根据引理 2, 将式 (33) 转化为:

$$\begin{aligned}p_2(t)\le&\frac{p_{11i}}{||\hat{\boldsymbol{z}}_{1i}||}(||\hat{\boldsymbol{z}}_{1i}||\cdot||\hat{\boldsymbol{z}}_{3i}||+||\hat{\boldsymbol{z}}_{1i}||\cdot||\boldsymbol{\varphi}_i(t,\boldsymbol{g}_i)||)+\\&\frac{p_{12i}}{||\hat{\boldsymbol{z}}_{1i}||}(||\hat{\boldsymbol{z}}_{2i}||\cdot||\hat{\boldsymbol{z}}_{3i}||+||\hat{\boldsymbol{z}}_{2i}||\cdot||\boldsymbol{\varphi}_i(t,\boldsymbol{g}_i)||)-\\&\frac{\epsilon p_{13i}}{||\hat{\boldsymbol{z}}_{1i}||}(\hat{\boldsymbol{z}}_{3i}^{\mathrm{T}}\hat{\boldsymbol{z}}_{3i}+||\hat{\boldsymbol{z}}_{3i}||\cdot||\boldsymbol{\varphi}_i(t,\boldsymbol{g}_i)||)\end{aligned}\tag{34}$$

根据引理 3, 可构造:

$$\begin{cases}||\hat{\boldsymbol{z}}_{1i}||\cdot||\hat{\boldsymbol{z}}_{3i}||\le c_{4i}\hat{\boldsymbol{z}}_{1i}^{\mathrm{T}}\hat{\boldsymbol{z}}_{1i}+\dfrac{1}{4c_{4i}}\hat{\boldsymbol{z}}_{3i}^{\mathrm{T}}\hat{\boldsymbol{z}}_{3i},\ c_{4i}>0\\ ||\hat{\boldsymbol{z}}_{1i}||\cdot||\boldsymbol{\varphi}_i||\le c_{5i}\hat{\boldsymbol{z}}_{1i}^{\mathrm{T}}\hat{\boldsymbol{z}}_{1i}+\dfrac{1}{4c_{5i}}\boldsymbol{\varphi}_i^{\mathrm{T}}\boldsymbol{\varphi}_i,\ c_{5i}>0\\ ||\hat{\boldsymbol{z}}_{2i}||\cdot||\hat{\boldsymbol{z}}_{3i}||\le c_{6i}\hat{\boldsymbol{z}}_{2i}^{\mathrm{T}}\hat{\boldsymbol{z}}_{2i}+\dfrac{1}{4c_{6i}}\hat{\boldsymbol{z}}_{3i}^{\mathrm{T}}\hat{\boldsymbol{z}}_{3i},\ c_{6i}>0\\ ||\hat{\boldsymbol{z}}_{2i}||\cdot||\boldsymbol{\varphi}_i||\le c_{7i}\hat{\boldsymbol{z}}_{2i}^{\mathrm{T}}\hat{\boldsymbol{z}}_{2i}+\dfrac{1}{4c_{7i}}\boldsymbol{\varphi}_i^{\mathrm{T}}\boldsymbol{\varphi}_i,\ c_{7i}>0\\ ||\hat{\boldsymbol{z}}_{3i}||\cdot||\boldsymbol{\varphi}_i||\le c_{8i}\hat{\boldsymbol{z}}_{3i}^{\mathrm{T}}\hat{\boldsymbol{z}}_{3i}+\dfrac{1}{4c_{8i}}\boldsymbol{\varphi}_i^{\mathrm{T}}\boldsymbol{\varphi}_i,\ c_{8i}>0\end{cases}\tag{35}$$

联立式 (34)、(35), 可得:

$$p_2(t)\le\frac{1}{||\hat{\boldsymbol{z}}_{1i}||}\hat{\boldsymbol{z}}_i^{\mathrm{T}}(Y_{2i}(\epsilon)+Z_{2i}(\epsilon))\hat{\boldsymbol{z}}_i\tag{36}$$

其中, $d_4=\frac{p_{11i}}{4c_{4i}}+\frac{p_{12i}}{4c_{6i}}-\epsilon p_{13i}(1+c_{8i})$,

$$Y_{2i}(\epsilon)=\begin{bmatrix}p_{11i}(c_{4i}+c_{5i}) & 0 & 0\\ 0 & p_{12i}(c_{6i}+c_{7i}) & 0\\ 0 & 0 & d_4\end{bmatrix}\otimes\boldsymbol{I}_3$$

$$Z_{2i}(\epsilon)=\left(\frac{p_{11i}}{4c_{5i}}+\frac{p_{12i}}{4c_{7i}}-\frac{\epsilon p_{13i}}{4c_{8i}}\right)\begin{bmatrix}\delta_i^2 & 0 & 0\\ 0 & 0 & 0\\ 0 & 0 & 0\end{bmatrix}\otimes\boldsymbol{I}_3$$

联立式 (31)、(32)、(36), 可得:

$$\begin{cases}\dot{V}_{20i}(t,\epsilon)\le-\dfrac{1}{||\hat{\boldsymbol{z}}_{1i}||}(\hat{\boldsymbol{z}}_i^{\mathrm{T}}\bar{W}_i(\epsilon)\hat{\boldsymbol{z}}_i)-\hat{\boldsymbol{z}}_i^{\mathrm{T}}\bar{X}_i(\epsilon)\hat{\boldsymbol{z}}_i\\ \bar{W}_i(\epsilon)=W_i(\epsilon)\otimes\boldsymbol{I}_3,\ \bar{X}_i(\epsilon)=X_i(\epsilon)\otimes\boldsymbol{I}_3\end{cases}\tag{37}$$

其中,

$$W_i(\epsilon)=\begin{bmatrix}w_{11}+\epsilon\tilde{w}_{11} & * & *\\ w_{21} & w_{22} & *\\ w_{31}+\epsilon\tilde{w}_{31} & w_{32}+\epsilon\tilde{w}_{32} & w_{33}+\epsilon\tilde{w}_{33}\end{bmatrix}$$

$$X_i(\epsilon)=\begin{bmatrix}x_{11} & * & *\\ x_{21} & x_{22} & *\\ x_{31}+\epsilon\tilde{x}_{31} & x_{32}+\epsilon\tilde{x}_{32} & \epsilon\tilde{x}_{33}\end{bmatrix}$$

由式 (37) 可知: $W_i(\epsilon)>0$, $X_i(\epsilon)>0$ 时, $\dot{V}_{20i}(t,\epsilon)<0$ 成立.

由引理 4, 可知:

$$\begin{cases}\lambda_{\min}(P_{2i})||\hat{\boldsymbol{z}}_i||^2\le\hat{\boldsymbol{z}}_i^{\mathrm{T}}P_{2i}(\epsilon)\hat{\boldsymbol{z}}_i\le\lambda_{\max}(P_{2i})||\hat{\boldsymbol{z}}_i||^2\\ \lambda_{\min}(\bar{W}_i)||\hat{\boldsymbol{z}}_i||^2\le\hat{\boldsymbol{z}}_i^{\mathrm{T}}\bar{W}_i(\epsilon)\hat{\boldsymbol{z}}_i\le\lambda_{\max}(\bar{W}_i)||\hat{\boldsymbol{z}}_i||^2\\ \lambda_{\min}(\bar{X}_i)||\hat{\boldsymbol{z}}_i||^2\le\hat{\boldsymbol{z}}_i^{\mathrm{T}}\bar{X}_i(\epsilon)\hat{\boldsymbol{z}}_i\le\lambda_{\max}(\bar{X}_i)||\hat{\boldsymbol{z}}_i||^2\end{cases}\tag{38}$$

基于式 (38), 可得:

$$\begin{cases}||\hat{\boldsymbol{z}}_{1i}||\le||\hat{\boldsymbol{z}}_i||\le\dfrac{(\boldsymbol{z}_i^{\mathrm{T}}P_{2i}(\epsilon)\boldsymbol{z}_i)^{\frac{1}{2}}}{\lambda_{\min}^{\frac{1}{2}}(\hat{P}_{2i})}\\ ||\hat{\boldsymbol{z}}_i||^2\ge\dfrac{\boldsymbol{z}_i^{\mathrm{T}}P_i(\epsilon)\boldsymbol{z}_i}{\lambda_{\max}(P_i)},\ ||\hat{\boldsymbol{z}}_i||^2\le\dfrac{\boldsymbol{z}_i^{\mathrm{T}}X_i(\epsilon)\boldsymbol{z}_i}{\lambda_{\min}(\hat{X}_i)}\end{cases}\tag{39}$$

根据式 (37)、(39), 可得:

$$\begin{aligned}\dot{V}_{20i}(t,\epsilon)\le&-\frac{1}{||\hat{\boldsymbol{z}}_{1i}||}\lambda_{\min}(\bar{W}_i)||\hat{\boldsymbol{z}}_i||^2-\\&\lambda_{\min}(\bar{X}_i)\cdot||\hat{\boldsymbol{z}}_i||^2\le-r_{2i}V_{20i}^{\frac{1}{2}}(t,\epsilon)-r_{3i}V_{20i}(t,\epsilon)\end{aligned}\tag{40}$$

其中, $r_{2i}=\frac{\lambda_{\min}^{\frac{1}{2}}(P_{2i})\lambda_{\min}(\bar{W}_i)}{\lambda_{\max}(P_{2i})}$, $r_{3i}=\frac{\lambda_{\min}(\bar{X}_i)}{\lambda_{\max}(P_{2i})}$.

将式 (40) 代入式 (30), 可得:

$$\begin{aligned}\dot{V}_{2i}(t,\epsilon)\le&-r_{2i}V_{20i}^{\frac{1}{2}}(t,\epsilon)-r_{3i}V_{20i}(t,\epsilon)+\frac{1}{\gamma_{1i}}\cdot\\&(\alpha_i(t)-\hat{\alpha}_i)\dot{\alpha}_i(t)+\frac{1}{\gamma_{2i}}(\beta_i-\hat{\beta}_i)\dot{\beta}_i(t)=\\&\frac{1}{\gamma_{2i}}(\beta_i(t)-\hat{\beta}_i)\dot{\beta}_i(t)-r_{2i}V_{20i}^{\frac{1}{2}}(t,\epsilon)-\\&\frac{b_{2i}}{\sqrt{2\gamma_{2i}}}|\beta_i(t)-\hat{\beta}_i|-\frac{b_{1i}}{\sqrt{2\gamma_{1i}}}|\alpha_i(t)-\hat{\alpha}_i|-\\&\frac{b_{3i}}{2\gamma_{1i}}|\alpha_i(t)-\hat{\alpha}_i|^2-\frac{b_{4i}}{2\gamma_{2i}}|\beta_i(t)-\hat{\beta}_i|^2+\\&\frac{b_{1i}}{\sqrt{2\gamma_{1i}}}|\alpha_i(t)-\hat{\alpha}_i|+\frac{b_{2i}}{\sqrt{2\gamma_{2i}}}|\beta_i(t)-\hat{\beta}_i|+\\&\frac{b_{3i}}{2\gamma_{1i}}|\alpha_i(t)-\hat{\alpha}_i|^2+\frac{b_{4i}}{2\gamma_{2i}}|\beta_i(t)-\hat{\beta}_i|^2+\\&\frac{1}{\gamma_{1i}}(\alpha_i(t)-\hat{\alpha}_i)\dot{\alpha}_i(t)-r_{3i}V_{20i}(t,\epsilon)\end{aligned}\tag{41}$$

根据柯西不等式[28], 将式 (41) 转化为:

$$\begin{aligned}\dot{V}_{2i}(t,\epsilon)\le&-\check{r}_{2i}V_{2i}^{\frac{1}{2}}(t,\epsilon)-\check{r}_{3i}V_{2i}(t,\epsilon)-\\&|\alpha_i(t)-\hat{\alpha}_i|\left(\frac{1}{\gamma_{1i}}\dot{\alpha}_i(t)-\frac{b_{3i}b_{5i}}{2\gamma_{1i}}-\frac{b_{1i}}{\sqrt{2\gamma_{1i}}}\right)-\\&|\beta_i(t)-\hat{\beta}_i|\left(\frac{1}{\gamma_{2i}}\dot{\beta}_i(t)-\frac{b_{4i}b_{6i}}{2\gamma_{2i}}-\frac{b_{2i}}{\sqrt{2\gamma_{2i}}}\right)\end{aligned}\tag{42}$$

其中, $\check{r}_{2i}=\min(r_{2i},b_{1i},b_{2i})$, $\check{r}_{3i}=\min(r_{3i},b_{3i},b_{4i})$.

令式 (42) 中 $\frac{1}{\gamma_{1i}}\dot{\alpha}_i(t)-\frac{b_{3i}b_{5i}}{2\gamma_{1i}}-\frac{b_{1i}}{\sqrt{2\gamma_{1i}}}=0$, $\frac{1}{\gamma_{2i}}\dot{\beta}_i(t)-\frac{b_{4i}b_{6i}}{2\gamma_{2i}}-\frac{b_{2i}}{\sqrt{2\gamma_{2i}}}=0$, 可得:

$$\dot{\alpha}_i(t)=b_{1i}\sqrt{\frac{\gamma_{1i}}{2}}+\frac{b_{3i}b_{5i}}{2},\ \dot{\beta}_i(t)=b_{2i}\sqrt{\frac{\gamma_{2i}}{2}}+\frac{b_{4i}b_{6i}}{2}$$

则式 (42) 可转化为:

$$\dot{V}_{2i}(t,\epsilon)\le-\check{r}_{2i}V_{2i}^{\frac{1}{2}}(t,\epsilon)-\check{r}_{3i}V_{2i}(t,\epsilon)\tag{43}$$

结合式 (30)、(43), 根据柯西不等式[28], 可得:

$$\begin{aligned}\dot{\bar{V}}(t,\epsilon)\le&\sum_{i=1}^{m}(-\check{r}_{2i}V_{2i}^{\frac{1}{2}}(t,\epsilon)-\check{r}_{3i}V_{2i}(t,\epsilon))\le\\&-\check{r}_{2k}\bar{V}^{\frac{1}{2}}(t,\epsilon)-\check{r}_{3k}\bar{V}(t,\epsilon)\end{aligned}\tag{44}$$

其中, $\check{r}_{2k}=\min(\check{r}_{2i})$, $\check{r}_{3k}=\min(\check{r}_{3i})$.

即在改进型自适应 STW 滑模控制器 (26) 的作用下, 无人机集群系统的误差有限时间内稳定. □

4　一致性误差收敛时间分析

在本节, 我们将比较自适应多尺度 STW 算法和改进型自适应多尺度 STW 算法的收敛时间, 进一步分析改进型算法具有更短的收敛时间的原因. 在控制器 (8) 的作用下, 根据式 (25), 可得:

$$\dot{V}(t,\epsilon)\le-\check{r}_kV^{\frac{1}{2}}(t,\epsilon)\tag{45}$$

假定状态 $\boldsymbol{z}_i$ 在 t_{r1} 时刻收敛, 将式 (45) 两边同乘 $\frac{\mathrm{d}t}{V^{\frac{1}{2}}(t,\epsilon)}$, 并在 $[t_0,t_{r1}]$ 上进行积分:

$$\begin{cases}\displaystyle\int_{V(t_0,\epsilon)}^{V(t_{r1},\epsilon)}\frac{\mathrm{d}V(t,\epsilon)}{V^{\frac{1}{2}}(t,\epsilon)}\le\int_{t_0}^{t_{r1}}-\check{r}_k\mathrm{d}t\\V^{\frac{1}{2}}(t_{r1},\epsilon)-V^{\frac{1}{2}}(t_0,\epsilon)\le-\check{r}_k(t_{r1}-t_0)\end{cases}\tag{46}$$

其中, $t_0=0$, 状态 $\boldsymbol{z}_i$ 在 t_{r1} 时刻收敛, 即 $V^{\frac{1}{2}}(t_{r1},\epsilon)=0$, 代入式 (46) 可得:

$$t_{r1}\le\frac{2V^{\frac{1}{2}}(t_0,\epsilon)}{\check{r}_k}\tag{47}$$

在控制器 (26) 的作用下, 由式 (44) 可得:

$$\dot{\bar{V}}(t,\epsilon)\le-\check{r}_{2k}\bar{V}^{\frac{1}{2}}(t,\epsilon)-\check{r}_{3k}\bar{V}(t,\epsilon)\tag{48}$$

假定状态 $\hat{\boldsymbol{z}}_i$ 在 t_{r2} 时刻收敛, 将式 (48) 两边同乘 $\frac{\mathrm{d}t}{\check{r}_{2k}\bar{V}^{\frac{1}{2}}(t,\epsilon)+\check{r}_{3k}\bar{V}(t,\epsilon)}$, 并在 $[t_0,t_{r2}]$ 上进行积分:

$$\begin{cases}\displaystyle\int_{\bar{V}(t_0,\epsilon)}^{\bar{V}(t_{r2},\epsilon)}\frac{1}{\check{r}_{2k}\bar{V}^{\frac{1}{2}}(t,\epsilon)+\check{r}_{3k}\bar{V}(t,\epsilon)}\mathrm{d}\bar{V}(t,\epsilon)\le\\\displaystyle\qquad\int_{t_0}^{t_{r2}}-1\mathrm{d}t\\f(t_{r2})-f(t_0)\le-(t_{r2}-t_0)\end{cases}\tag{49}$$

其中, $t_0=0$, $f(t)=\frac{2}{\check{r}_{3k}}\ln(1+\frac{\check{r}_{3k}\bar{V}^{\frac{1}{2}}(t,\epsilon)}{\check{r}_{2k}})$. 状态 $\hat{\boldsymbol{z}}_i$ 在 t_{r2} 时刻收敛, 即 $\bar{V}(t_{r2},\epsilon)=0$, 则 $\ln(1+\frac{\check{r}_{3k}\bar{V}^{\frac{1}{2}}(t_{r2},\epsilon)}{\check{r}_{2k}})=0$, 代入式 (49), 可得:

$$t_{r2}\le\frac{2}{\check{r}_{3k}}\ln\frac{\check{r}_{3k}\bar{V}^{\frac{1}{2}}(t_0,\epsilon)+\check{r}_{2k}}{\check{r}_{2k}}\tag{50}$$

由式 (47)、(50) 可知, 在改进型自适应 STW 滑模控制器 (26) 的作用下, 收敛时间与 $\ln(\cdot)$ 函数相关联, 由于 $\ln(\cdot)$ 函数的取对数特性, 使得无人机集群系统的一致性收敛时间更短, 即 $t_{r2}<t_{r1}$.

5　仿真分析

为验证所建立模型与控制律的有效性, 本次仿真选择了三个四旋翼无人机智能体集群, 三个智能体之间的交互关系由无向图表示, 且 $a_{12}=1$, $a_{13}=2$, $a_{23}=3$. 无人机间的连接方式可参照图 1.

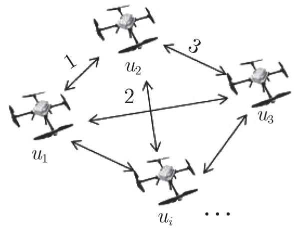

图 1　四旋翼无人机多智能体

Fig.1　The multi-agent of quadrotors

四旋翼无人机绕机体坐标系的转动惯量为: $I_{x1}=I_{y1}=6.22\times10^{-3}\ \mathrm{kg\cdot m^2}$, $I_{z1}=1.12\times10^{-3}\ \mathrm{kg\cdot m^2}$, $I_{x2}=I_{y2}=l9.22\times10^{-3}\ \mathrm{kg\cdot m^2}$, $I_{z2}=2.12\times10^{-3}\ \mathrm{kg\cdot m^2}$, $I_{x3}=I_{y3}=3.22\times10^{-3}\ \mathrm{kg\cdot m^2}$, $I_{z3}=7.12\times10^{-4}\ \mathrm{kg\cdot m^2}$. 四旋翼无人机的电动机和桨叶的转动惯量为: $J_{r1}=6\times10^{-5}\ \mathrm{kg\cdot m^2}$, $J_{r2}=9\times10^{-5}\ \mathrm{kg\cdot m^2}$, $J_{r3}=3\times10^{-5}\ \mathrm{kg\cdot m^2}$. 四旋翼无人机的空气摩擦阻力矩系数为: $k_{ax1}=k_{ay1}=k_{az1}=1.2\times10^{-4}\ \mathrm{N\cdot s/m}$, $k_{ax2}=k_{ay2}=k_{az2}=2.2\times10^{-4}\ \mathrm{N\cdot s/m}$, $k_{ax3}=k_{ay3}=k_{az3}=7.2\times10^{-5}\ \mathrm{N\cdot s/m}$, 取 $\epsilon=7.12\times10^{-4}$.

四旋翼无人机初始姿态角与角速度为:

$$\begin{cases} \boldsymbol{x}_1(0) = [0.5 \quad 1 \quad 5]^{\mathrm{T}} \\ \boldsymbol{v}_1(0) = [-0.2 \quad -0.5 \quad -15]^{\mathrm{T}} \\ \boldsymbol{x}_2(0) = [0.3 \quad 0.5 \quad 3]^{\mathrm{T}} \\ \boldsymbol{v}_2(0) = [-0.1 \quad 0.1 \quad 0.2]^{\mathrm{T}} \\ \boldsymbol{x}_3(0) = [-1 \quad -1 \quad 1]^{\mathrm{T}} \\ \boldsymbol{v}_3(0) = [0.1 \quad 0.5 \quad 1]^{\mathrm{T}} \end{cases}$$

跟踪系数 $l_1 = 1$, 非线性项中 $w_{ri} = 5\sin(t)$, 跟踪姿态角 $\boldsymbol{x}_0(t) = (\frac{\pi}{4}\sin(t), \frac{\pi}{4}\sin(t), \frac{\pi}{4}\sin(t) + \frac{\pi}{2})^{\mathrm{T}}$.

为了实现无人机的姿态角的同步, 仿真中采用了两种控制器对无人机姿态集群系统进行控制:

1) 采用自适应多尺度 STW 控制器 (8), 对应的控制器相关参数为: $b_{11} = 2$, $b_{12} = 2.2$, $b_{13} = 2.4$, $b_{21} = 1$, $b_{22} = 1.2$, $b_{23} = 1.4$, $\gamma_{11} = 2$, $\gamma_{12} = 3$, $\gamma_{13} = 4$. $p_{11} = -p_{22} = p_{31} = 1$, $p_{12} = -p_{22} = p_{32} = 1.2$, $p_{13} = -p_{23} = p_{33} = 1.4$. 自适应增益 $\beta_i(t)$, $\alpha_i(t)$ 形式如式 (11) 所示.

2) 采用改进型自适应多尺度 STW 控制器 (26), 对应的控制器相关参数为: $k_{11} = 1$, $k_{12} = 1.1$, $k_{13} = 1.2$, $k_{21} = 2$, $k_{22} = 2.1$, $k_{23} = 2.2$. $b_{3i} = 0.1$, $b_{4i} = 0.1$, $b_{5i} = 8$, $b_{6i} = 8$. $b_{21} = 1$, $b_{22} = 1.2$, $b_{23} = 1.4$, $\gamma_{21} = 1$, $\gamma_{22} = 2$, $\gamma_{23} = 3$. 自适应增益 $\beta_i(t)$, $\alpha_i(t)$ 为:

$$\dot{\alpha}_i(t) = b_{1i}\sqrt{\frac{\gamma_{1i}}{2} + \frac{b_{3i}b_{5i}}{2}},\ \dot{\beta}_i(t) = b_{2i}\sqrt{\frac{\gamma_{2i}}{2} + \frac{b_{4i}b_{6i}}{2}}$$

图 2 为在自适应多尺度 STW 控制器 (8) 作用下的四旋翼无人机的姿态角状态轨迹曲线. 从中可以看出无人机集群系统的姿态角在有限时间内实现状态同步. 图 2(d) 为自适应增益变化曲线, 可以看出, 自适应增益持续增加直至无人机姿态角协同. 图 3 表明: 在改进型自适应多尺度 STW 控制器 (26) 作用下, 也能够使得无人机集群系统姿态角在有限时间内达到一致. 两种控制算法下系统的性能指标如表 1 所示, 主要从平均收敛时间、平均稳态误差这两个指标进行比较. 由表 1 可知, 在改进型自适应多尺度 STW 算法控制下的无人机集群系统的快速性明显增加, 准确性略微减弱. 相对于文献 [30] 提出的控制算法, 本文提出的这两种算法在收敛时间上更短, 控制的准确性更高.

6 结论

本文针对四旋翼无人机系统中具有的多时间尺度特性, 以及存在未知边界非线性的问题, 设计了一种自适应多尺度 STW 滑模算法. 将无人机快慢系统“分而治之”, 实现了分尺度精确控制. 并且通过该算法在有效削减滑模动态抖振的同时, 还保证了无人机集群系统在有限时间内的一致性. 本文还

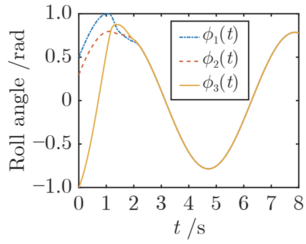

(a) 无人机横滚角变化曲线
(a) Quadrotors roll angle change curve

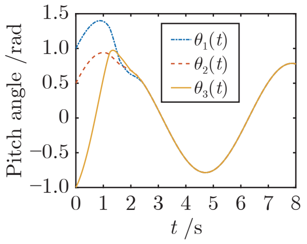

(b) 无人机俯仰角变化曲线
(b) Quadrotors pitch angle change curve

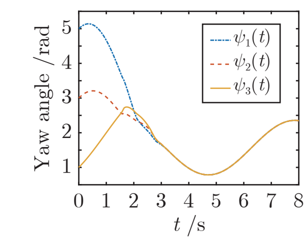

(c) 无人机偏航角变化曲线
(c) Quadrotors yaw angle change curve

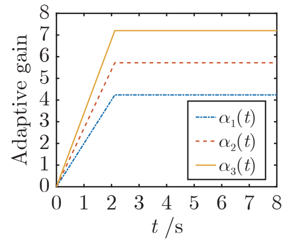

(d) 自适应增益 $\alpha_i(t)$ 变化曲线
(d) Adaptive gain $\alpha_i(t)$ variation curve

图 2 自适应多尺度 STW 算法控制下的无人机姿态历时曲线

Fig.2 Trajectories of attitudes under the adaptive multi-scale STW controller

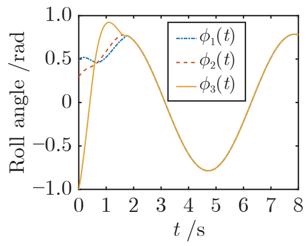

(a) 无人机横滚角变化曲线
(a) Quadrotors roll angle change curve

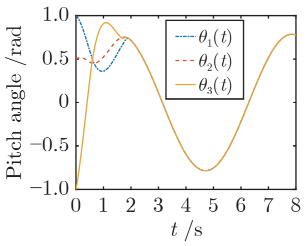

(b) 无人机俯仰角变化曲线
(b) Quadrotors pitch angle change curve

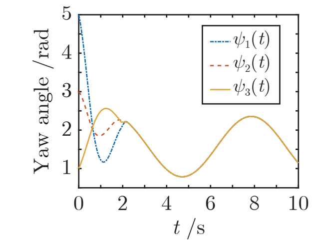

(c) 无人机偏航角变化曲线
(c) Quadrotors yaw angle change curve

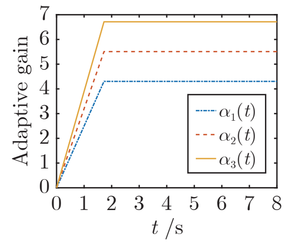

(d) 自适应增益 $\alpha_i(t)$ 变化曲线
(d) Adaptive gain $\alpha_i(t)$ variation curve

图 3 改进型自适应多尺度 STW 算法控制下的无人机姿态历时曲线

Fig.3 Trajectories of attitudes under the modified adaptive multi-scale STW controller

表 1 四旋翼无人机姿态角系统性能指标
Table 1 Performance index of a quadrotor′s attitude system

	平均收敛时间 (s)	平均稳态误差 (rad)
STW 滑模算法	2.587	1.76×10^{-7}
改进型 STW 滑模算法	1.947	3.56×10^{-7}
文献 [30] 中的算法	10.870	4.24×10^{-6}

设计了一种改进型自适应多尺度 STW 滑模算法, 增加了系统的快速性. 最后通过仿真验证了两种控制方法的有效性, 实现了无人机集群系统的姿态协同.

References

1 Xu J, Fridman E, Fridman L, Niu Y G. Static sliding mode control of systems with arbitrary relative degree by using artificial delays. *IEEE Transactions on Automatic Control*, 2020, **65**(12): 5464−5471

2 Xu Jing, Cai Chen-Xiao, Li Yong-Qi, Zou Yun. Dual-loop path tracking and control for quad-rotor miniature unmanned aerial vehicles. *Control Theory & Applications*, 2015, **32**(10): 1335−1342
(许璟, 蔡晨晓, 李勇奇, 邹云. 小型四旋翼无人机双闭环轨迹跟踪与控制. 控制理论与应用, 2015, **32**(10): 1335−1342)

3 Zhou Xiao-Cheng, Yan Jian-Gang, Xie Yu-Peng, Zhai Hong-Jun. Task distributed algorithmic for multi-UAV based on auction mechanism. *Journal of Naval Aeronautical and Astronautical University*, 2012, **27**(3): 308−312
(周小程, 严建钢, 谢宇鹏, 翟鸿君. 多无人机对地攻击任务分配算法. 海军航空工程学院学报, 2012, **27**(3): 308−312)

4 Chang Yi-Zhe, Li Zhan-Wu, Yang Hai-Yan, Luo Wei-Ping, Xu An. A decision-making for multiple target attack based on characteristic of future long-range cooperative air combat. *Fire Control & Command Control*, 2015, **40**(6): 36−40
(常一哲, 李战武, 杨海燕, 罗卫平, 徐安. 未来中远距协同空战多目标攻击决策研究. 火力与指挥控制, 2015, **40**(6): 36−40)

5 Luo C, Yu L J, Ren P. A vision-aided approach to perching a bioinspired unmanned aerial vehicle. *IEEE Transactions on Industrial Electronics*, 2018, **65**(5): 3976−3984

6 De Castro A I, Torres-Sanchez J, Pena J M, Jimenez-Brenes F M, Csillik O, Lopez-Granados F. An automatic random forest-OBIA algorithm for early weed mapping between and within crop rows using UAV imagery. *Remote Sensing*, 2018, **10**(2): Article No. 285

7 Kim B O, Yun K H, Chang T S, Bahk J J, Kim S P. A preliminary study on UAV photogrammetry for the hyanho coast near the military reservation zone, eastern coast of Korea. *Ocean and Polar Research*, 2017, **39**(2): 159−168

8 Wang Ning, Wang Yong. Fuzzy uncertainty observer based adaptive dynamic surface control for trajectory tracking of a quadrotor. *Acta Automatica Sinica*, 2018, **44**(4): 685−695
(王宁, 王永. 基于模糊不确定观测器的四旋翼飞行器自适应动态面轨迹跟踪控制. 自动化学报, 2018, **44**(4): 685−695)

9 Vallejo D, Castro-Schez J J, Glez-Morcillo C, Albusac J. Multi-agent architecture for information retrieval and intelligent monitoring by UAVs in known environments affected by catastrophes. *Engineering Applications of Artificial Intelligence*, 2020, **87**: Article No. 103243

10 Xie Hai-Jun, Liang Zhan-Min, Wang Jian. Design and implementation of control system of UAV formation performance. *Electronic Design Engineering*, 2021, **29**(17): 75−79
(谢海军, 梁湛民, 王健. 无人机编队表演控制系统设计与实现. 电子设计工程, 2021, **29**(17): 75−79)

11 Yang Ming-Yue, Shou Ying-Xin, Tang Yong, Liu Chang, Xu Bin. Multi-Quadrotor UAVs formation maintaining and collision avoidance control. *Acta Aeronautica et Astronautica Sinica*, 2022, **43**: 1−11
(杨明月, 寿莹鑫, 唐勇, 刘畅, 许斌. 多四旋翼无人机编队保持与避碰控制. 航空学报, 2022, **43**: 1−11)

12 Mao X, Zhang H, Wang Y. Flocking of quad-rotor UAVs with fuzzy control. *ISA Transactions*, 2018, **74**: 185−193

13 Liu Ming-Wei, Gao Bing-Bing, Wang Peng-Fei, Liu Ya-Nan, Li Yi-Meng, Li Pei-Qi. Research on UAV formation obstacle avoidance flight based on neural network adaptive PID control. *Unmanned Systems Technology*, 2022, **5**(2): 22−32
(刘明威, 高兵兵, 王鹏飞, 刘亚南, 李怡萌, 李沛琦. 基于神经网络自适应 PID 的无人机编队避障飞行控制研究. 无人系统技术, 2022, **5**(2): 22−32)

14 Li Xi-Kang, Xu Jing, Niu Yu-Gang. Memory proportional-integral-retarded output sliding mode controller design. *Control Theory & Applications*, 2022, **3**: 1−9
(李习康, 许璟, 牛玉刚. 带记忆比例−积分−时滞输出滑模控制器设计. 控制理论与应用, 2022, **3**: 1−9)

15 Tian Bo-Lin, Li Pin-Pin, Lu Han-Chen, Zong Qun. Trajectory and attitude coordinated control of multiple unmanned aerial vehicles in complex environments. *Acta Aeronautica et Astronautica Sinica*, 2020, **41**: 36−43
(田栢苓, 李品品, 鲁瀚辰, 宗群. 复杂环境下多无人机轨迹姿态协同控制. 航空学报, 2020, **41**: 36−43)

16 Yu Z Q, Liu Z X, Zhang Y M, Qu Y H, Su C Y. Decentralized fault-tolerant cooperative control of multiple UAVs with prescribed attitude synchronization tracking performance under directed communication topology. *Frontiers of Information Technology & Electronic Engineering*, 2019, **20**(5): 685−701

17 Xi Wen-Long, Tang Wen-Xiu, Xu Li-Shang, Liu Fang-Yue. Position control of DC-motor based on one-order low pass filter backstepping sliding mode method. *Chongqing University of Posts and Telecommunications*, 2017, **29**(4): 550−556
(奚文龙, 唐文秀, 许李尚, 刘方悦. 基于一阶低通滤波器滑模反步法的直流电机位置控制. 重庆邮电大学学报 (自然科学版), 2017, **29**(4): 550−556)

18 Liu Z, Lou X, Jia J. Event-triggered dynamic output-feedback control for a class of Lipschitz nonlinear systems. *Frontiers of Information Technology & Electronic Engineering*, 2022, **23**(11): 1684−1699

19 Chen Zai-Fa, Liu Yan-Cheng. Control of permanent magnet synchronous motor based on super spiral sliding model variable structure. *Motor and Control Applications*, 2017, **44**(6): 19−23
(陈再发, 刘彦呈. 基于超螺旋滑模变结构永磁同步电机的控制. 电机与控制应用, 2017, **44**(6): 19−23)

20 Ren Yan, Wang Yi-Min, Niu Zhi-Qiang, Xiao Yong-Jian. Application of high-order terminal sliding mode control in stable platform. *Control Engineering*, 2021, **28**(3): 553−558
(任彦, 王义敏, 牛志强, 肖永健. 高阶终端滑模控制在稳定平台中的应用. 控制工程, 2021, **28**(3): 553−558)

21 Derafa L, Benallegue A, Fridman L. Super twisting control algorithm for the attitude tracking of a four rotors UAV. *Journal of the Franklin Institute*, 2012, **349**(2): 685−699

22 Naidu D. Singular perturbations and time scales in control theory and applications: An overview. *Dynamics of Continuous Discrete and Impulsive Systems Series B*, 2002, **9**: 233−278

23 Li F, Zheng W X, Xu S Y, Yuan D M. A novel ε-dependent Lyapunov function and its application to singularly perturbed systems. *Automatica*, 2021, **133**: Article No. 109749

24 He Shou-Yuan. Properties and judgment methods of positive definite matrix. *Journal of Mathematical and Chemical Problem Solving*, 2020, **24**: 18−19
(何守元. 正定矩阵的性质及判定方法. 数理化解题研究, 2020, **24**: 18−19)

25 Malamud S M. A converse to the Jensen inequality, its matrix extensions and inequalities for minors and eigenvalues. *Linear Algebra and Its Applications*, 2001, **22**(1): 19−41

26 Shtessel Y B, Moreno J A, Plestan F. Super-twisting adaptive

sliding mode control: A Lyapunov design. In: Proceedings of the 49th Conference on Decision and Control. Petersburg, Russia: IEEE, 2010. 5109−5113

27 Wang G L, Li Z Q, Miao X, Zhang Q L, Yang C Y. Fault detection of discrete-time delay Markovian jump systems with delay term modes partially available. *Journal of the Franklin Institute*, 2019, **356**(5): 3045−3071

28 Hu Xiao-Li, Qiao Long-Kun. Improvement of Cauchy′s inequality and its application. *Journal of Jianghan University*, 2021, **49**(6): 29−33
(胡晓莉, 乔龙坤. 柯西不等式的改进及其应用. 江汉大学学报, 2021, **49**(6): 29−33)

29 Munoz F, Estrada M B, González-Hernández I, Salazar S, Lozano R. Super twisting vs modified super twisting algorithm for altitude control of an unmanned aircraft system. In: Proceedings of the 12th International Conference on Electrical Engineering, Computing Science and Automatic Control. Tu Delft, Netherlands: IEEE, 2015. 1−6

30 Jin Wan-Li, Yu Zhi-Yong, Jiang Hai-Jun. Leader-following consensus of second-order multi-agent systems via event-triggered impulsive control. *Journal of Lanzhou University of Technology*, 2022, **48**(5): 153−160
(金琬丽, 于志永, 蒋海军. 事件触发脉冲控制下二阶多智能体系统的领导跟随一致性. 兰州理工大学学报, 2022, **48**(5): 153−160)

蔡运颂 华东理工大学信息科学与工程学院硕士研究生. 主要研究方向为滑模控制, 多智能体和无人机控制.
E-mail: y30210956@mail.ecust.edu.cn
(**CAI Yun-Song** Master student at the College of Information Science and Engineering, East China University of Science and Technology. His research interest covers sliding mode control, multi-agent, and UAV control.)

许 璟 华东理工大学信息科学与工程学院副教授. 主要研究方向为高阶滑模观测与控制, 无人机系统建模与控制, 智能优化算法和人工智能技术. 本文通信作者.
E-mail: jingxu@ecust.edu.cn
(**XU Jing** Associate professor at the College of Information Science and Engineering, East China University of Science and Technology. Her research interest covers high-order sliding mode observation and control, UAV system modeling and control, intelligent arithmetic optimization, and artificial intelligence technology. Corresponding author of this paper.)

牛玉刚 华东理工大学信息科学与工程学院教授. 主要研究方向为随机控制系统, 滑模控制, 无线传感网络和微电网能量管理.
E-mail: acniuyg@ecust.edu.cn
(**NIU Yu-Gang** Professor at the College of Information Science and Engineering, East China University of Science and Technology. His research interest covers stochastic control system, sliding mode control, wireless sensor network, and microgrid energy management.)